# Quantum Lattice Dynamical Effects on the Single-Particle Excitations in 1D Mott and Peierls Insulators

H. Fehske[1], G. Wellein[2], G. Hager[2], A. Weiße[3], & A. R. Bishop[4]

[1]Ernst-Moritz-Arndt-Universität Greifswald, [2]Friedrich-Alexander-Universität Erlangen,
[3]University of New South Wales (Australia) & [4]Los Alamos National Laboratory (U.S.A.)

*Abstract:* As a generic model describing quasi-one-dimensional Mott and Peierls insulators, we investigate the Holstein-Hubbard model for half-filled bands using numerical techniques. Combining Lanczos diagonalization with Chebyshev moment expansion we calculate exactly the photoemission and inverse photoemission spectra and use these to establish the phase diagram of the model. While polaronic features emerge only at strong electron-phonon couplings, pronounced phonon signatures, such as multi-quanta band states, can be found in the Mott insulating regime as well. In order to corroborate the Mott to Peierls transition scenario, we determine the spin and charge excitation gaps by a finite-size scaling analysis based on density-matrix renormalization group calculations.

## Introduction

The one-dimensional (1D) Holstein-Hubbard model (HHM) has been used extensively to describe for novel low-dimensional materials, e.g., conjugated polymers, organic charge transfer salts or halogen-bridged transition metal complexes, and the associated metal-insulator and insulator-insulator transitions The HHM accounts for a tight-binding electron band, intra-site Coulomb repulsion between electrons of opposite spin, and a local coupling of the charge carriers to the phonon system:

$$H = -t\sum_{i,\sigma}(c^\dagger_{i\sigma}c_{i+1\sigma} + \text{H.c.}) + U\sum_i n_{i\uparrow}n_{i\downarrow} \\ -\sqrt{\varepsilon_p\omega_0}\sum_{i,\sigma}(b^\dagger_i + b_i)n_{i\sigma} + \omega_0\sum_i b^\dagger_i b_i\,.$$

The physics of the HHM is governed by the competition between electron itinerancy ($\propto W = 4t$) on the one hand and electron-electron ($\propto u = U/4t$) and electron-phonon ($\propto \lambda = \varepsilon_p/2t$) interactions on the other hand, which both tend to immobilize the charge carriers. At least for the half-filled band case Mott insulator (MI) or Peierls insulator (PI) states are expected to be favored over the metallic state at $T = 0$. The correlated MI shows pronounced spin-density-wave (SDW) fluctuations but has continuous symmetry. It therefore exhibits no long-range order in 1D. In contrast the PI is characterized by dominant charge-density-wave (CDW) correlations and true long-range order because a discrete symmetry is broken. While the gaps to both spin ($\Delta_s$) and charge ($\Delta_c$) excitations are finite in the PI, the spin gap vanishes in the 1D MI, which is related to spin charge separation.

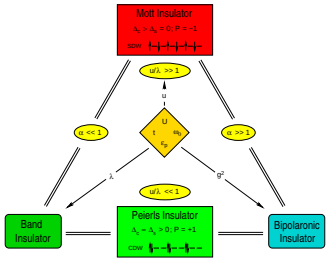


*Fig. 1: Schematic phase diagram of the Holstein-Hubbard model at half-filling.*

In a strict sense these results hold in the adiabatic limit ($\omega_0 = 0$) for "$U$-only" (Hubbard model) and "$\lambda$-only" (Peierls model) parameters. At finite phonon frequency and $U = 0$ (Holstein model) a critical electron-phonon (EP) coupling is required to set up the CDW phase. Depending on the adiabaticity ratio $\alpha = \omega_0/t$ the PI represents a traditional band insulator ($\alpha \ll 1$) or a bipolaronic insulator ($\alpha \gg 1$, $g^2 \gg 1$). Although for the more general HHM the situation is much less clear, we expect that the features of the insulating phase will depend markedly on the ratio of Coulomb and EP interactions $u/\lambda$, allowing for quantum phase transitions between insulating phases. For finite periodic chains, the MI-PI quantum phase transition could be identified by a ground-state level crossing associated with a change in the parity eigenvalue $P$. /1,2/

## Numerical results and discussion

We begin by studying the spectral density of single-particle excitations associated with the injection of a spin-$\sigma$ electron with wave number $K$, $A^+_{K\sigma}(\omega)$ (inverse photoemission (IPE)), and the corresponding quantity for the emission of an electron, $A^-_{K\sigma}(\omega)$ (photoemission (PE)), where

$$A^\pm_{K\sigma}(\omega) = \sum_m |\langle\psi^{(N_{el}\pm1)}_m|c^\pm_{K\sigma}|\psi^{(N_{el})}_0\rangle|^2 \\ \times\delta[\omega \mp (E^{(N_{el}\pm1)}_m - E^{(N_{el})}_0)]$$

with $c^+_{K\sigma} = c^\dagger_{K\sigma}$ and $c^-_{K\sigma} = c_{K\sigma}$. The spectral function $A_{K\sigma}(\omega) = A^+_{K\sigma}(\omega) + A^-_{K\sigma}(\omega)$ obeys various sum rules and allows for a connection to angle-resolved photoemission spectroscopy (ARPES). The ED results presented for $A^\pm_{K\sigma}(\omega)$ in the following were obtained for an eight-site system with periodic boundary conditions.

Let us first consider the MI regime (Fig. 2). The most prominent feature we observe in the MI regime is the opening of a gap at $K = \pm\pi/2$, indicating massive charge excitations. A comparison with the pure Hubbard model classifies this gap as the Mott-Hubbard correlation gap. Its value $\Delta/t \simeq 3.25$ almost coincides with the optical gap $\Delta_{opt}$. The dispersion of the lower (upper) Hubbard band can be derived tracing the uppermost (lowest) excitations in each $K$ sector. As a result of the coupling to the phonon system the electronic levels in each $K$ sector split, creating phonon side bands. The distinct peaks are separated by multiples of the bare phonon frequency and can be assigned to relaxation processes of the $Q = 0$ phonon modes. Interestingly, mediated by $Q \neq 0$ phonons, there appear "shadows" of the band belonging to a dominant electronic excitation in a certain $K$ sector in other $K$ sectors, giving rise to a weak "breather-like" excitation [3], which is almost dispersionless in the Brillouin zone.

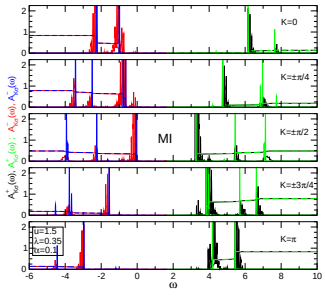


*Fig. 2: Wave-number-resolved spectral densities for photoemission ($A^-_{K\sigma}(\omega)$; red lines) and inverse photoemission ($A^+_{K\sigma}(\omega)$; black lines) in the MI state ($u/\lambda \gg 1$). The corresponding integrated densities $S^\pm_{K\sigma}(\omega)$ are given by dashed lines. Data for the pure Hubbard model (blue and green lines) were shifted by $-(\varepsilon_p N^2_{el}/N)$ and included for comparison.*

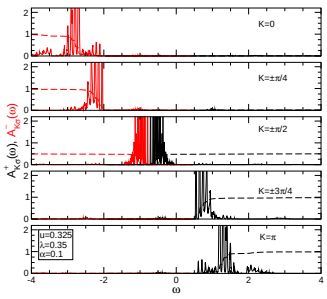


*Fig. 3: PE (red lines) and IPE (black lines) spectra near the MI-PI transition point ($u \simeq \lambda$).*

If we decrease the Hubbard interaction at fixed EP coupling strength the Mott-Hubbard gap weakens and finally closes at about $(u/\lambda)_c \simeq 1$, which marks the MI-PI crossover (see Fig. 3). Approaching the critical point from above and below, the ground state and the first excited state become degenerate. These states have different eigenvalues $P$ of the site-inversion operator $Pc^\dagger_{i\sigma}P^\dagger = c^\dagger_{N-i\,\sigma}$ ($i = 0,\ldots,N-1$) and we have verified that the ground-state site parity is $P = +1$ in the MI and $P = -1$ in the PI. Obviously the critical point is characterized by gapless charge excitations at the Fermi momenta but should not be considered as metallic because the Drude weight is ill-defined. [2]

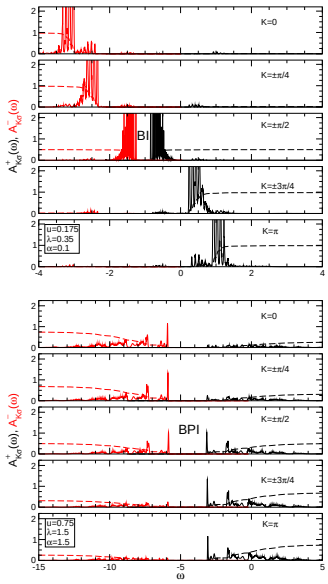


*Fig. 4: PE and IPE spectra in the Peierls phase ($u \ll \lambda$). The upper (lower) panels show typical results obtained for the band insulator (BI) at $\alpha \ll 1$ and bipolaronic insulator (BPI) at $\alpha \gg 1$.*

If the Hubbard interaction is further reduced, a CDW accompanied by a dimerization of the lattice develops. As a result the electronic band structure becomes gapped again (see Fig. 4 (upper panel)). The form of the spectra, however, is quite different from MI case. While in the MI regime the lowest peak in each $K$ sector is clearly the dominant one, in the BI phase rather broad (I)PE signatures appear. Within these excitation bands the spectral weight is almost uniformly distributed, which is a clear signature of multi-phonon absorption and emission processes that accompany every single-particle excitations in the PI. The lineshape then reflects the (Poisson-like) distribution of the phonons in the ground state. Again low-intensity "shadow bands" become visible. The situation changes radically if the insulating behavior is associated with localized bipolarons forming a CDW state (see Fig. 4, lower panel). Due to strong polaronic effects an almost flat band dispersion results with exponentially small (electronic) quasiparticle weight. Now the dominant peaks in the incoherent part of the (I)PE spectra are related to multiples of the (large) bare phonon frequency broadened by electronic excitations.

Since many-body gaps to excited states form the basis for making contact with experimentally measurable excitation gaps and also can be used to characterize different phases of the HHM, we determine the charge and spin gaps using DMRG:

$$\Delta_c = E^{(N+1)}_0(\tfrac{1}{2}) + E^{(N-1)}_0(-\tfrac{1}{2}) - 2E^{(N)}_0(0)\,, \\ \Delta_s = E^{(N)}_0(1) - E^{(N)}_0(0)\,.$$

$\Delta_c$ and $\Delta_s$ are finite in the PI and will converge further as $N \to \infty$. [4] Both gaps seem to vanish at the quantum phase transition point of the HHM with finite-frequency phonons, but in the critical region the finite-size scaling is extremely delicate. In the MI we found a finite charge excitation gap, which in the limit $u/\lambda \gg 1$ scales to the optical gap of the Hubbard model, whereas the extrapolated spin gap remains zero.

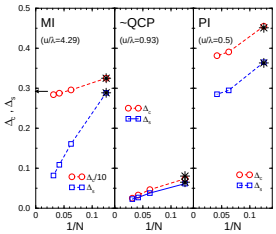


*Fig.5: DMRG finite-size scaling of spin- and charge excitation gaps in the HHM ($\lambda = 0.35$, $\alpha = 0.1$). Stars represent the ED results for the eight-site system. The arrow marks the value of the optical gap $\Delta_{opt}$ for the 1D Hubbard model. Since in our parallel DMRG program a pseudosite representation is used [5], the accessible system sizes are smaller at larger $\lambda/u$, where an increasing number of (phononic) pseudosites is required to reach convergence with respect to the phonons.*

As can be seen from Fig. 6, the staggered charge- and spin-structure factors,

$$S_c(\pi) = \frac{1}{N^2}\sum_{\substack{i,j\\ \sigma\sigma'}}(-1)^{|i-j|}\langle(n_{i\sigma}-\tfrac{1}{2})(n_{j\sigma'}-\tfrac{1}{2})\rangle, \\ S_s(\pi) = \frac{1}{N^2}\sum_{i,j}(-1)^{|i-j|}\langle S^z_i S^z_j\rangle,\ S^z_i = \frac{1}{2}\sum_\sigma n_{i\sigma},$$

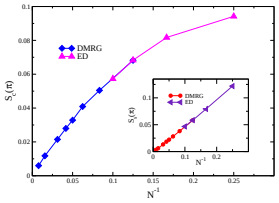


*Fig. 6: Finite-size scaling study of spin and charge structure factors at $q = \pi$ in the half-filled 1D HHM with periodic BCs at $u = 1$, $\lambda = 1$, and $\alpha = 1$ with five boson pseudosites, $m = 1000$ and $N$ up to 128.*

are strongly suppressed approaching the quantum critical point from below and above, respectively. The DMRG results obtained for a sequence of systems with up to 128 sites can be used to perform a reliable finite-size extrapolation: At the quantum critical point $S_c(\pi)$ and $S_s(\pi)$ vanish in the thermodynamic limit $N \to \infty$.

*Conclusions:* To summarize, we have presented a comprehensive picture of the physical properties of the 1D half-filled finite-phonon frequency Holstein-Hubbard model. With respect to the metal the electron-electron coupling favors the Mott insulating state whereas the electron-phonon interaction is responsible for the Peierls insulator to occur. The PI typifies a band insulator in the adiabatic weak-to-intermediate coupling range or a bipolaronic insulator for non-to-antiadiabatic strong-coupling. Our results for the single-particle spectra and spin/charge excitation gaps give clear indication of a Mott- to Peierls-insulator quantum phase transition at $u/\lambda \simeq 1$. Quantum phonon dynamics yields pronounced effects in the (I)PE spectra, which might be of great importance for interpreting photoemission experiments of low-dimensional strongly correlated electron-phonon systems such as MX-chain compounds.

**Some references:**
/1/ H. Fehske *et al.*, Physica B **312-313**, 562 (2002); Eur. Phys. J. B **31**, 11 (2003).
/2/ Ph. Brune *et al.*, arXiv:cond-mat/0304697.
/3/ W. Z. Wang *et al.*, PRL **80**, 3284 (1998).
/4/ S. R. Manmana *et al.*, arXiv:cond-mat/0307741.
/5/ G. Hager *et al.*, J. Comp. Phys., accepted (2003).